I－B 283

SYNTHESIS OF STRONG GROUND MOTION FOR THE 1891 NOBI EARTHQUAKE

Nippon KOEI R&D Center　Member　○ H. DARAMA, T. OHSUMI
Miyazaki University, Civil Eng. Dept.　Member　Prof. T. HARADA

1. Introduction: The Nobi earthquake of October 28, 1891 [M8.0; Muramatu, 1962] is the largest inland type ever recorded in the Japanese Islands, by causing extremely strong ground motion and heavy seismic damage (X-XII on the Modified Mercalli scale). It resulted in the only known remarkable surface fault break which could be clearly traced (Nukumi-Neodani-Umehara Faults) as long as 80 km with maximum horizontal and vertical displacements of 8 m and 3 m respectively. The reported damage in and around the epicenter area was: 7,273 people dead (17,175 injured), 142,177 houses collapsed (80,184 damaged), and over 10,000 landslide incidents observed [Usami,1966]. Our aim by proceeding this study is to predict seismic ground motions that would be expected to arise from future earthquakes of comparable magnitude and with a similar mechanism to that of Nobi earthquake fault system. Especially, we focused on determining the effects of directivity for the strong-motion time duration [Ben-Menahem, 1961]. In order to carry out and synthesize the main event, we employed a stochastic simulation technique so called EGF method. This method is based on spectral representation of stochastic waves in making use of kinematic source model with ω^2 property and the representation theorem of elastodynamics of far-field seismic waves.

2. Faulting and rupture modeling: Number of Seismological and Geological studies were performed after this unique earthquake and various results have been reported to date so far. According to the founding, rupture initiated at a depth near the northwestern end of the Nikumi fault, and propagated southeastward almost unilaterally along pre-existing active faults with velocities of 2.2-2.5 km/sec, forming successive conjugate set of left-lateral strike-slip faults which were termed as Nobi fault system (Fig.1). The largest surface fault displacement and damages were observed around Midori-Kinbara along the Neodani fault. The released stresses are estimated to be 40-150 bars, which considerably differs from one place to another. All of the strong motion over the entire length was estimated as being completed within 40 sec. Old type strong-motion seismographs at Gifu, Nagoya, Osaka and Tokyo, recorded the Nobi earthquake. Unfortunately, the records of first two stations are now available with only the initial portion of ground motion. The records went off scale probably due to the arrival of large amplitude S-waves. Estimated displacement at Gifu is 34 cm as that of 23 in Nagoya [Omori, 1894]. Recently, the probable existence of blind-trust faults during the 1891 event, was revealed on the basis of the seismicity, topography pattern, and leveling surveys [F.Pollitz, 1994]. However, in simulation, we will refer to the faults model and source parameters (Fig.2) proposed by Mikumo&Ando, 1976-[1].

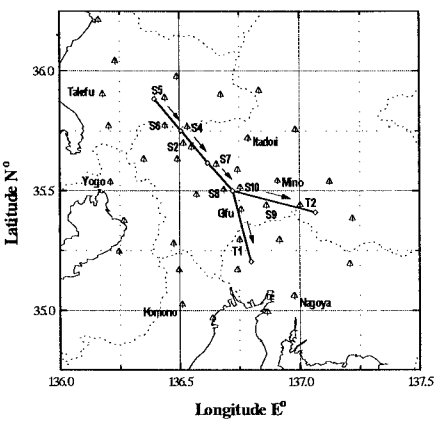

Fig.1 Location of the Nobi fault system and target sites.

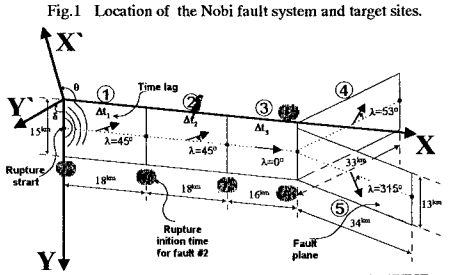

N°	E°	d(km)	θ(°)	λ(°)	δ(°)	τ(sec)	L(km)	W(km)	U(cm)
① 35.884	136.393	0	145	45	90	1.0	18	15	140
② 35.751	136.507	0	145	45	90	2.0	18	15	425
③ 35.618	136.621	0	145	0	90	3.5	16	15	700
④ 35.500	136.723	0	107	53	90	1.5	33	15	250
⑤ 35.500	136.723	2	163	315	90	1.0	34	13	140

Fig.2. Fault models and source parameters proposed by Mikumi&Ando, 1976.

3. Stochastic simulation by EGF: According to the theorem, far-field displacement $u(x,\omega)$ in a homogeneous, isotropic and layered medium can be expressed in the following integral and approximate final form over finite fault model [Aki&Richards,1980]. Eq.(1) indicates that the simulated motion of large fault is summation of contributions with weight $T_{mn}(\omega)$ from $N_L \times N_W$ small faults. This means that an approximate simulation method can be obtained, using a single observation record $u_o(x,\omega)$ due to the $(m_o n_o)^{th}$ fault. Transfer function $T_{mn}(\omega)$, which is used in this study, was proposed by Harada, 1995-[2], as a generalized form of

$$u(\tilde{x},t)=\sum_{m=1}^{N_L}\sum_{n=1}^{N_W}\int_{\xi_m}^{\xi_m+\Delta L}\int_{\eta_n}^{\eta_n+\Delta W}\dot{D}(\xi_m,\eta_n,t-\tau_{mn})*G(\tilde{x},\xi_m,\eta_n,t-t_{mn})d\xi\,d\eta \xrightarrow{FFT} u(\tilde{x},\omega)\cong\sum_{m=1}^{N_L}\sum_{n=1}^{N_W}\frac{R_0}{R_{mn}}T_{mn}(\omega)e^{-i\omega(\tau_{mn}+t_{mn})}u_0(\tilde{x},\omega) \quad ...(1)$$

Irikura's formulation as shown at Eq.(2). The synthesis of a non-stationary small event was generated by a stochastic

$$T_{mn}(\omega)=\left[\frac{\omega^2+\left(\frac{N}{\tau}\right)^2}{\omega^2+\left(\frac{1}{\tau}\right)^2}\right]\left[\frac{i\omega-\left(\frac{1}{\tau}\right)}{i\omega-\left(\frac{N}{\tau}\right)}\right]\left[\frac{1+\kappa\left(\frac{\omega\tau}{2}\right)^2}{1+\left(\frac{\omega\tau}{2}\right)^2}\right],\ N=\left(\frac{M_o}{m_o}\right)^{\frac{1}{3}},\ \tau_{mn}=\frac{\zeta_{mn}}{V_R},\ t_{mn}=\frac{R_{mn}-R}{V_S},\ u_o(\tilde{x},\omega)\to u(\tilde{x},\omega|\tau,\kappa,V_R,V_S) \quad ...(2)$$

point source model with ω^2 property as indicated by Eq.(3) [Shinozuka et al., 1987]. Source-station geometry, or directivity, is involved in our simulation as being a key parameter (azimuth) to determine the effective time duration

[Harada et al., 1997]-[3] together with empirical relations of Ohsaki (1994).

$$a(t)=\sqrt{2}\sum_{j=1}^{N_\omega}\sqrt{2S_{aa}(t,\omega_j)\Delta\omega}\;\cos(\omega_j t+\phi_j)\;;\;\omega_j=j\Delta\omega\;;\;\Delta\omega=\frac{\omega_u}{N_\omega}\;;\;j=1,2,\ldots,N_\omega\;;\;|A(\omega)|=CA_S(\omega)A_D(\omega)A_A(\omega)$$

$$S_{aa}(t,\omega)=\frac{1}{2\pi T_e}|W(t)|^2|A(\omega)|^2\;;\;\phi_j[0,2\pi]_1^{N_t}\;;\;T_e=T_c-T_b\leftarrow\begin{vmatrix}T_b=[0.12-0.04(M-7)T_d]\\T_c=[0.50-0.04(M-7)T_d]\end{vmatrix}\leftarrow T_d=2.63T_f \qquad ...(3)$$

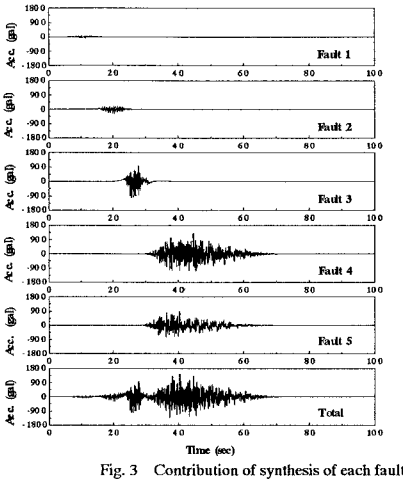

M(dyne.cm)	Δσ(bar)	φ(°)	Δ(km)	κ()	t_e(sec)
① 1.134x10²⁶	40	-2.5	61.2	3	0.0
② 3.442x10²⁶	75	-3.2	43.2	3	10.18
③ 5.040x10²⁶	150	-5.0	25.2	3	20.36
④ 3.712x10²⁶	75	-50.5	9.3	3	26.76
⑤ 1.856x10²⁶	75	10.5	9.3	3	26.76

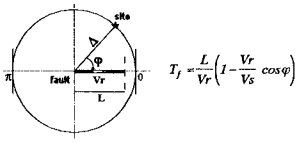

Fixed parameters

Sampling (dt-sec.)	0.03
Rupture Vel. (Vr-km/sec)	2.50
Shear Vel. (Vs-km/sec)	3.70
Density (ρ-t/m³)	2.70
Natu. Freq. (ω_g-rad/sec)	15.6
Damping (h_g)	0.6
Freq. Atenu. (q_1,q_2)	0.5 - 2.3

Fig. 3 Contribution of synthesis of each fault time history at target Gufi site

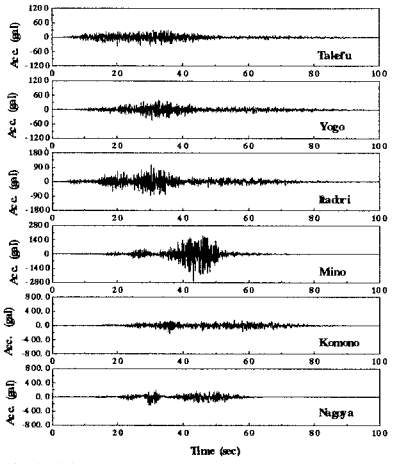

Fig. 4 Wave forms of selected sites around the Nobi area.

4. Concluding remarks: The synthetic acceleration time history of ground motion was successfully generated over 40 target stations, using the prescribed stochastic EGF method. Faults are individually simulated, and contributions from each of them are finally summed at target site, in order to get the total time history (Fig.3). We have observed that the rupture duration depends not only on the rupture velocity and the dimensions of the fault itself, but also the orientation of the observation station relative to the fault (azimuth) as well. Directivity, or focusing energy along the fault in the direction of the rupture, is a significant factor for most of the large earthquakes, including Nobi event. Briefly, shaking intensity decreases much more rapidly perpendicular to the fault rupture plane than along the fault axis (Fig. 4). According to the results of our simulation, we have obtained very high acceleration values, especially along the Neodani-③ fault, exceeding well over 2g. For the duration time of the total motion, generally, a value over 40 sec was observed, which is consistent with the literature. As can be seen from the (Fig.5), fault displacements gradually increased during the rupture propagation through NW-SE. Highest surface displacement was obtained near the southern end of Neodani fault at site S8, with having a value of 221 cm. As for a comparison, in simulation, we got 98 cm displacement at Gifu as 27 in Nagoya, which is again close to the values obtained by previous researchers and estimated ones by field observations after the main event. Finally, this numerical example, prove the effectiveness of approach and demonstrate the effects of the directivity on the synthesis of acceleration time histories.

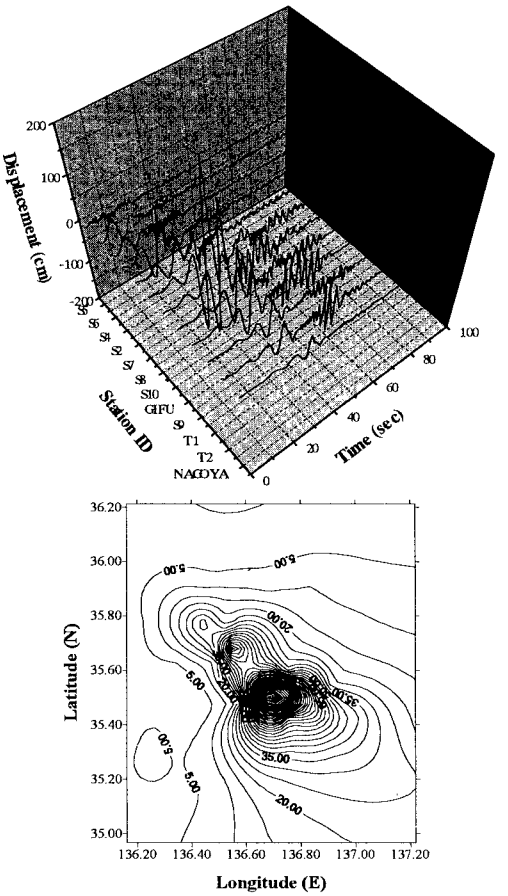

Fig. 5 Displacement time histories of selected sites and entire contour plot along the fault system.

5. References:

[1] Mikumo T., Ando M., *A search into the faulting mechanism of the 1891 great Nobi Earthquake,* Journal of Physics of the Earth, Vol. 24, 63-87, 1976.

[2] Harada T., *Digital simulation of Earthquake ground motions using seismological model* Proceeding of JSCE, No.507, I-30, pp.209-217,1995.

[3] Harada T., Ohsumi T., Darama H., *Engineering simulation of ground motions using seismological model.* (ICOSSAR '97), Nov. 24-28, Kyoto